

Magnetism at the Ni(001) surface: A high-precision, all-electron local-spin-density-functional study

E. Wimmer* and A. J. Freeman

Physics Department, Northwestern University, Evanston, Illinois 60201

H. Krakauer

Physics Department, College of William and Mary, Williamsburg, Virginia 23185

(Received 25 July 1983; revised manuscript received 27 February 1984)

We present the results of high-precision, all-electron, self-consistent local-spin-density-functional calculations on a seven-layer Ni(001) film using the full-potential linearized-augmented-plane-wave method. It is found that the surface atoms have a magnetic moment which is enhanced by almost 20% compared with the bulklike atoms in the interior of the film. There is no indication of a Friedel-type oscillation in the layer-by-layer magnetic moments. Although the negative core-contact spin densities for the surface atoms are enhanced in magnitude by 20%, the contribution from the (4s-derived) valence electrons changes sign and becomes slightly positive in the surface layer. This causes a net decrease in magnitude of the total contact spin density by 20%. In agreement with photoemission experiments we find the majority-spin \bar{M}_3 surface state to be occupied, contrary to the early results of Wang and Freeman for a nine-layer film and to recently presented results obtained by Jepsen *et al.* on a five-layer film. The work function is found to be 5.37 eV, in good agreement with the experimental value of 5.22 ± 0.04 eV. For the core levels of the surface atoms we obtain a shift between 0.3 and 0.5 eV towards reduced binding energies which is explained in terms of *d*-band narrowing and layer-by-layer charge neutrality.

I. INTRODUCTION

During the past decade, Ni has become one of the most studied transition metals because of its intriguing electronic and magnetic properties, its technological importance as a catalyst, and its wide applicability in metallurgy and in materials science. Thus the investigation and the microscopic understanding of bulk and surface properties of Ni continues to be a fascinating challenge for new experimental and theoretical techniques.

In particular, the existence of magnetically dead layers on the Ni surface has been a matter of controversy (cf. the references given by Jepsen *et al.*¹ and Krakauer *et al.*²), but there is now general agreement that there are no magnetically dead layers on the clean Ni(100) and Ni(110) surfaces. Rather, theoretical-computational studies on these surfaces^{1,2} have revealed a slight enhancement of the magnetic moments in the surface layer compared with that in bulk Ni. Recently, this prediction has been confirmed experimentally by Feder *et al.*³ using spin-polarized low-energy electron diffraction. Furthermore, the understanding of photoemission data for Ni cannot be considered to be complete⁴ as far as *d*-band width, exchange splitting, spin-polarization reversal, and the assignment of surface states⁵ are concerned.

Since the original calculation of the electronic and magnetic structures of the Ni(100) surface by Wang and Freeman (WF),⁶ considerable progress has been made in improving the accuracy of surface electronic structure calculations. Nevertheless, even the most recent theoretical-computational studies reported^{1,2} for the Ni surfaces use approximations not inherent in the local-spin-density-functional (LSDF) theory.⁷⁻¹⁰ So, for example, only

five-layer slabs have been treated self-consistently by Jepsen *et al.*¹ and Krakauer *et al.*² and in both cases^{1,2} the full potential is not included rigorously. *A priori*, it is not clear to which extent these approximations influence the results for delicate effects such as surface magnetism, and to which extent LSDF theory can be made responsible for any discrepancies with experiment. Thus the aim of the present work is to solve the LSDF problem for the Ni(001) surface as closely as possible to the LSDF limit. This is achieved within the single-slab approach for surfaces by using a seven-layer Ni(001) film and by solving the LSDF equations using the full-potential linearized-augmented-plane-wave (FLAPW) method,¹¹ one of the most accurate methods known today to calculate surface electronic structures.

II. METHODOLOGY AND COMPUTATIONAL ASPECTS

In the present calculation the Ni(001) surface is represented by a single slab of seven Ni layers. No surface relaxations are considered, and hence we have used throughout the slab the nearest-neighbor distances of bulk Ni corresponding to an fcc lattice constant of 6.6488 a.u., which is the same value as in our previous study.² For the exchange-correlation potential we employ the explicit form of von Barth and Hedin,⁹ which has also been used in the previous calculations on Ni(001).^{1,2,6} The LSDF one-particle equations for the seven-layer film are solved by means of a spin-polarized version¹² of the FLAPW method which is described in detail by Wimmer *et al.*¹¹ Because of the high density of states at the Fermi energy for the Ni system, attention has to be paid to an accurate

integration over the first Brillouin zone (BZ). Thus we have used a fine \vec{k} mesh of 45 \vec{k} points within $\frac{1}{8}$ of the first BZ and interpolated linearly by means of a triangular method, the two-dimensional equivalent of the well-known tetrahedron method (see Ref. 6 and references therein). The eigenstates are sorted with respect to a mirror-reflection symmetry in the center of the film into even and odd states. For each symmetry type about 170 linearized augmented plane waves are used as a variational basis set corresponding to a maximum plane-wave kinetic energy of 9.7 Ry. The self-consistency procedure has been accelerated by using the scheme of Anderson¹³ as suggested by Hamann¹⁴ alternating with conventional attenuated feedback. It is interesting to note that due to the high density of states at the Fermi level the Ni system is numerically rather unstable and a straight mixing of more than 2% output charge density to the input density gives rise to a diverging charge oscillation between the center of the film and the surfaces. On the other hand, the spin densities, due to the absence of long-range Coulomb effects, can be mixed rather generously (up to 50%) which greatly accelerates the convergence of the spin densities including those at the nuclei. A total of about 50 iterations was needed to converge the charge densities to better than $0.5 \times 10^{-3} e/(\text{a.u.})^3$ average deviation between input and output density. This corresponds to an average deviation in the corresponding potentials of better than 4.5 mRy. By then the spin density was converged in the average (including core) to better than $0.3 \times 10^{-3} e/(\text{a.u.})^3$ and the eigenvalues to better than 0.5 mRy.

The core electrons are treated fully relativistically with the same assumption as in our previous study² for including spin polarization. The valence electrons are calculated semirelativistically, i.e., without spin-orbit coupling. Since the spin-orbit splitting of the atomic Ni 3d states is about three times smaller than the theoretical exchange splitting in bulk Ni, it is believed that the scalar-relativistic treatment of the valence electrons does not influence the spin density substantially and thus does not affect the results concerning the changes of the magnetization in the surface layer compared with the interior of the Ni crystal.

III. RESULTS

A. Charge densities

Figure 1 shows the total charge density in the upper half of a seven-layer Ni film. It can be seen (Fig. 1) that the screening length for the charge density at the metal-vacuum interface is essentially only one atomic layer: already the subsurface atoms ($S-1$) exhibit a bulklike environment in the charge density. This is particularly obvious from the low-density regions between the atoms. It is remarkable how well the charge densities in the interior of the film agree with those obtained in the earlier calculation⁶ where a quite different technique has been used to solve the local spin-density-functional equations. In the low-density region at the vacuum side we obtain a corrugation which follows naturally the atomic positions of the atoms in the surface layer, whereas WF found for very

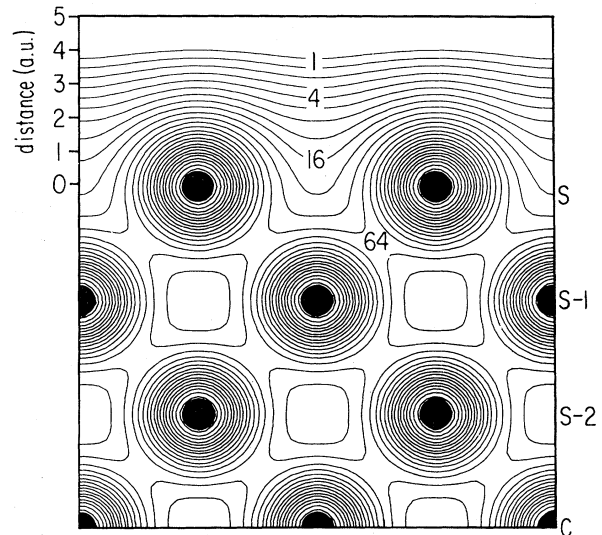


FIG. 1. Total electronic charge density of the upper half of a seven-layer Ni(001) film in the (110) plane perpendicular to the surface. The value of the lowest contour is $1 \times 10^{-3} e/(\text{a.u.})^3$ and subsequent contours differ by a factor of $\sqrt{2}$.

low densities (cf. the contour 1 in Fig. 6 of Ref. 6) a qualitatively different picture, presumably due to their method of constructing their charge density by superposing atomic, spherically symmetric densities. Figure 1 also clearly shows that the charge density at the metal-vacuum interface tends to smooth out the discrete nature of the surface determined by the arrangement of the atoms in the surface layer and thus the charge density contour lines become parallel to the surface only about 1 Å above the surface atoms.

A more detailed picture of the rearrangement of the electrons in the surface layer is obtained by partitioning the charge into contributions from different regions and by a further decomposition inside atomic spheres according to different l values as shown in Table I. From the total charges inside the spheres we see (Table I) that the surface atoms lose about 0.2 electronic charges into the vacuum. This spill-out determines in a delicate way the electrostatic surface dipole barrier and thus the work function.¹⁵ The work function is found to be 5.37 eV in good agreement with the experimental value^{16,17} of 5.22 ± 0.04 eV and the theoretical values obtained by Jepsen *et al.*¹ (5.4 eV) and Krakauer *et al.*² (5.5 eV) for the thinner films. As expected from the charge density map (Fig. 1) the charges inside the muffin-tin sphere of all atoms below the surface (i.e., $S-1$, $S-2$, and in the central layer, C) are essentially the same and equal to the bulklike value in the center of the film. Adding the charge in the vacuum to the charge in the surface layer (sphere plus interstitial) we find that the surface layer is in itself electrically neutral as is each layer below the surface. This observation is consistent with the short screening length of the changes in the charge density induced by the vacuum interface. The inspection of the l -projected charge components (Table I) reveals that the loss of electronic charge for the surface atoms is mostly due to a reduction of p -

TABLE I. Decomposition of the electronic valence charge in a seven-layer Ni(001) film. The charges inside the spheres of radii of 2.31501 a.u. are projected according to different l values. The small contributions from $l > 2$ are omitted, the film-vacuum boundary is assumed 2.3512 a.u. above the plane of the surface (S) atoms. $S-1$ and $S-2$ denote the first and second atomic layer below the surface atoms, and C labels the atoms in the center of the film.

	s	p	d	Sphere	Interstitial (vacuum)	Total in layer
S	0.43	0.29	8.29	9.03	0.83(0.14)	10.0
$S-1$	0.45	0.43	8.28	9.21	0.79	10.0
$S-2$	0.45	0.43	8.29	9.21	0.79	10.0
C	0.46	0.43	8.29	9.21	0.79	10.0

like charge and only a slight reduction in s -like charge. It is remarkable and important for the magnetic aspects discussed below that the amount of d -like charge persists essentially unchanged for the surface atoms. The reduction of p -like charge is clearly related to the reduced number of nearest neighbors in the surface layer: If one would continue to reduce the number of neighbors he would find a further reduction of p -like charge and in the limit of the free atom the $4p$ level would be unoccupied. Another way of looking at the reduction of p -like charge in the surface would be the argument that p orbitals would project quite far out into the vacuum (in contrast to the localized d orbitals) resulting in a rather pronounced corrugation of the charge density. Yet we observe, as mentioned above, a smoothening of the charge density in the vacuum thus making the occupation of p orbitals less favorable. It should be noted that the charge density in the interior of the film is rather close to the traditional muffin-tin form thus giving an illustrative example of why muffin-tin densities and potentials were (and still are) successfully used in so many calculations on densely packed systems such as fcc transition metals.

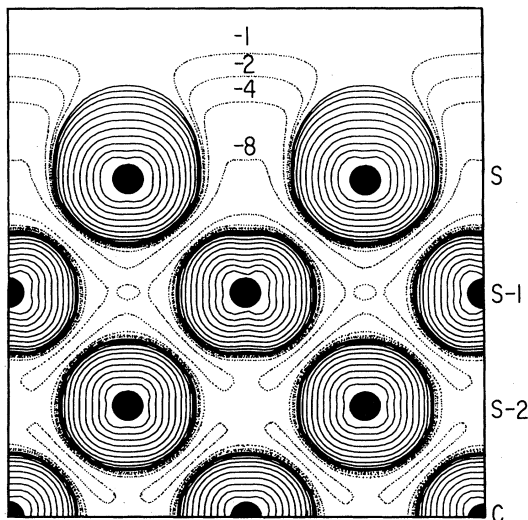


FIG. 2. Total spin density of the upper half of a seven-layer Ni(001) film in the (110) plane perpendicular to the surface. Regions of negative polarization are indicated by dotted contours. The value of the first positive contour (full line) is $1 \times 10^{-4} e/(\text{a.u.})^3$ and subsequent contours differ by a factor of 2.

B. Spin densities and magnetic moments

A contour plot (Fig. 2) of the self-consistent spin density reveals that, similar to the charge density (cf. Fig. 1), only one layer of surface atoms is markedly affected by the metal-vacuum interface and that obviously already the subsurface atoms ($S-1$) have essentially a bulklike spin density. For both the atoms in the interior and surface atoms the regions of strong positive polarization of the localized d electrons are separated by regions of negative polarization of the delocalized s, p electrons in between

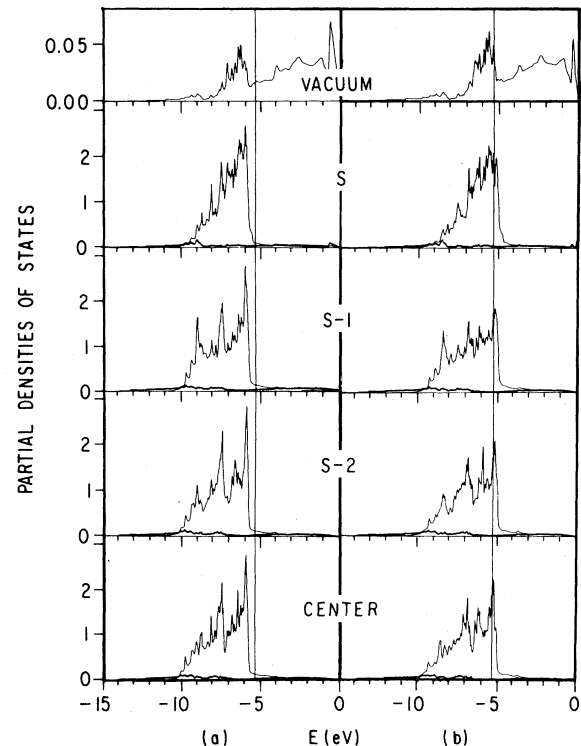


FIG. 3. Layer-projected and l -decomposed local densities of states of a seven-layer Ni(001) film in units of number of states per eV spin. (a) Majority and (b) the minority densities of states. The curves with a low density of states originate from the s - and p -like contributions inside the atomic spheres and the sharp structures arise from the d components. The "vacuum" region (top panels) designates the region outside the vacuum boundary which is assumed to be 2.3512 a.u. above the plane of the surface atoms.

TABLE II. Decomposition of the majority and minority valence charges in a seven-layer Ni(001) film. The same conventions as in Table I are used.

	<i>s</i>	<i>p</i>	<i>d</i>	Sphere	Interstitial (vacuum)	Total in layer
Majority						
<i>S</i>	0.21	0.14	4.50	4.87	0.41(0.07)	5.35
<i>S</i> - 1	0.22	0.21	4.46	4.91	0.38	5.29
<i>S</i> - 2	0.22	0.21	4.46	4.91	0.38	5.29
<i>C</i>	0.23	0.21	4.45	4.90	0.38	5.29
Minority						
<i>S</i>	0.22	0.15	3.79	4.17	0.43(0.07)	4.67
<i>S</i> - 1	0.23	0.22	3.82	4.29	0.40	4.69
<i>S</i> - 2	0.23	0.22	3.83	4.30	0.40	4.70
<i>C</i>	0.23	0.22	3.85	4.32	0.40	4.72

(cf. Fig. 3). This negative polarization of the delocalized *s,p* electrons projects out into the vacuum region. Thus an experimental technique which would allow a probe of the magnetization as one gradually approaches the surface from the vacuum would first show a negative polarization and then, as contributions from the positively polarized *d* electrons are picked up, the observed polarization should eventually change sign and become positive. It is tempting to interpret the electron-capture-spectroscopy measurements of Rau¹⁸ in this way: Rau¹⁸ observed that at a very small reflection angle (0.2°) the electron spin polarization on a Ni(001) surface was negative, but changed sign and became positive at larger angles (0.5° and 0.8°), i.e., for a closer approach to the surface. The spin densities are in the case of Ni, to a first approximation, a map of the occupied part at the top of the majority *d* band which has no occupied counterpart in the minority system. The change of the nonsphericity in the spin density for the surface atoms is therefore closely related to the surface-induced changes near the top of the *d* band. Hence we will return to this point in the discussions of the densities of states and the band structure in the following sections.

The spin density (Fig. 2) reveals a pronounced nonsphericity around the atomic sites in the interior of the system and a negative polarization in the interstitial region reaching a value of $-8 \times 10^{-4} e/(\text{a.u.})^3$, where this negative region projects out into the vacuum. As expected, the discrepancies between the present results and those obtained by WF (Ref. 6) are more severe for the spin density, being a difference of charge densities, than for the total charge density itself as mentioned in the preceding section.

In order to gain a deeper insight into the surface-induced charge rearrangements relevant for the surface magnetism we now analyze the decomposition of the charges of the majority and the minority valence electrons separately as was done for the total valence charge in the preceding section. One of the most important observations is (cf. Table II) that for the surface atoms the amount of majority *d*-like charge increases while the minority *d*-like charge decreases. As shown above (cf. Table I) the total *d*-like charge is the same for the surface atoms and the atoms in the interior. The *s*- and *p*-like charges in the different layers scale very similarly for the total valence charge and for that of the majority and the minority system individually (cf. Tables I and II). As a consequence, the spin imbalance is larger for the surface atoms than in the interior of the film. Thus the magnetic moment in the surface layer is enhanced compared with the bulklike interior (Table III). As expected, the dominant contribution to the magnetic moments originates from the localized *d*-like charges; the other contributions from the polarization of the *s*- and *p*-like electrons in the interstitial and the vacuum region represent only small corrections of the order of a few percent. The inspection of the layer-decomposed magnetic moments (Table III) give no significant indication of a Friedel-type oscillation of the magnetic moments. This finding is in contradiction to the results of WF, who report the following layer-projected magnetic moments for their nine-layer film (from the surface to the central layer): 0.44, 0.58, 0.62, 0.56, and $0.54\mu_B$. The corresponding results of the present seven-layer film calculation are (Table III) 0.68, 0.60, 0.59, and $0.56\mu_B$. Both calculations approach in the center of the film the experimental bulk value of $0.56\mu_B$.¹⁹

TABLE III. Decomposition of the magnetic moments (in μ_B) in a seven-layer Ni(001) film. The same conventions as in Table I are used.

	<i>s</i>	<i>p</i>	<i>d</i>	Sphere	Interstitial (vacuum)	Total in layer
<i>S</i>	-0.01	-0.01	0.72	0.70	-0.02(-0.005)	0.68
<i>S</i> - 1	-0.01	-0.02	0.64	0.62	-0.02	0.60
<i>S</i> - 2	-0.01	-0.02	0.63	0.61	-0.02	0.59
<i>C</i>	-0.00	-0.02	0.60	0.58	-0.02	0.56

TABLE IV. Electronic spin densities at the nuclei in a seven-layer Ni(001) film in units of $e/(\text{a.u.})^3$. The last column shows the ratio of the core spin density at the nuclear sites and the moment caused by the valence d electrons in the corresponding sphere.

	Core	core/ $\mu_B(d)$	Valence	Total in a.u.	Total in kG
S	-0.2000	0.279	+ 0.0056	-0.1944	-101.9
$S-1$	-0.1771	0.277	-0.0727	-0.2499	-131.0
$S-2$	-0.1746	0.277	-0.0577	-0.2323	-121.7
C	-0.1655	0.276	-0.0608	-0.2263	-118.6

The results of the present calculation together with the qualitatively similar results obtained for five-layer films^{1,2} indicate that a film of as little as five layers is sufficiently thick to describe adequately the magnetism on a surface such as Ni(001).

C. Contact spin densities at the nuclei

The electronic spin density at the nucleus is a key quantity for the interpretation of hyperfine interaction experiments which probe the coupling of the electronic spin to the nuclear magnetic moment. Theoretically, great care has to be taken to adequately describe this delicate quantity. In particular it is essential to describe not only the wave functions of the valence electrons at the nuclei accurately, but also to account for the dominant polarization of the core electrons. Thus an accurate all-electron method is needed which treats all electrons self-consistently. In a fully relativistic treatment the spin density at a nucleus originates from $s_{1/2}$ and the $p_{1/2}$ wave functions. The total spin density can be conveniently decomposed into the contribution from the valence electrons, i.e. in the case of Ni mainly from states which have 4s-like components near a given nucleus, and into contributions from the core electrons, i.e., in the present case from $1s$, $2s$, $2p_{1/2}$, $3s$, and $3p_{1/2}$ states.

Table IV shows that the total spin density at the nuclei in all layers are negative.²⁰ The magnitude is reduced, though, in the surface layer. The decomposition into contributions from core and valence electrons reveals that the core polarization (column 3 of Table IV) is always negative and scales very precisely with the moment of the d electrons in a given sphere²⁰ (cf. column 5 of Table IV). Owing to the increased d moment in the surface layer the core polarization in the surface layer is enhanced accordingly. However, the contribution from the valence electrons is found to change sign in the surface layer, i.e., to become positive. This important effect overrides the enhanced polarization of the core electrons and brings about the reduction in magnitude of the total spin density at the nuclei of surface atoms. Jepsen *et al.*¹ also reported a positive 4s contribution to the hyperfine field. However, since Jepsen *et al.*¹ used a frozen core density from an atomic calculation they were unable to provide an accurate total spin density at the nucleus. As shown by our results, the contribution from the core electrons is larger by a factor of about 4 than is the valence-electron contribution. In addition, the core polarization for surface atoms is substantially different from that of bulklike atoms (cf. Table IV).

D. Density of states

A convenient partition of the total density of states (DOS) consists in projecting out the contributions from each atomic sphere in each layer and by further decomposing according to different angular momentum quantum number thus obtaining atomic- and l -projected DOS as shown in Fig. 3. As expected, the DOS are dominated by the d bands which have in the bulklike center of the film a width of 5 eV and show for all layers except the surface layer great similarity with the DOS obtained for bulk Ni.²¹ The d band for the surface layer is markedly narrower and new states (between -6 and -7 eV for the majority states as shown in the left panels and between -5.5 and -6.5 eV for the minority states shown in the right panels of Fig. 3) make the DOS for the surface atoms less structured than in the bulk. It is also interesting to note that for the surface atoms the DOS near the bottom of the d band is clearly reduced as can be seen by inspecting the energy regions at -9 eV (majority) and -8.5 (minority) in Fig. 3. A comparison between the majority and the minority DOS reveals that the majority d bands are completely filled—a point which deserves further discussion in terms of the band structure—whereas the Fermi energy falls into a maximum of the minority DOS about 0.5 eV below the top of the minority d bands. We should note that a slight change in the structure of the minority DOS near the Fermi energy due to a fully relativistic treatment of the valence states could delicately influence the number of states at the Fermi energy.

The top panels in Fig. 3 show the part of the DOS which originates from states which project out into the vacuum region. Analysis shows that d -like surface states and surface resonance states are found near the top of the d bands for both the majority and the minority system. In addition, surface-induced states of free-electron-like character exist just below the vacuum level (which is set to zero). These states induce a structure in the s, p -like DOS of the surface atoms but not for atoms below.

E. Surface states and surface resonance states

In this section we present and discuss the one-particle energy spectrum of a seven-layer Ni(001) slab in terms of the most characteristic parts of the energy-band structure along the high-symmetry lines $\bar{\Delta}$, $(\bar{\Gamma}-\bar{X})$, \bar{Y} ($\bar{X}-\bar{M}$), and \bar{Z} ($\bar{M}-\bar{\Gamma}$) of the two-dimensional Brillouin zone (Fig. 4). It should be noted (cf. Fig. 4) that the two-dimensional surface unit cell for the Ni(001) surface is rotated by 45°

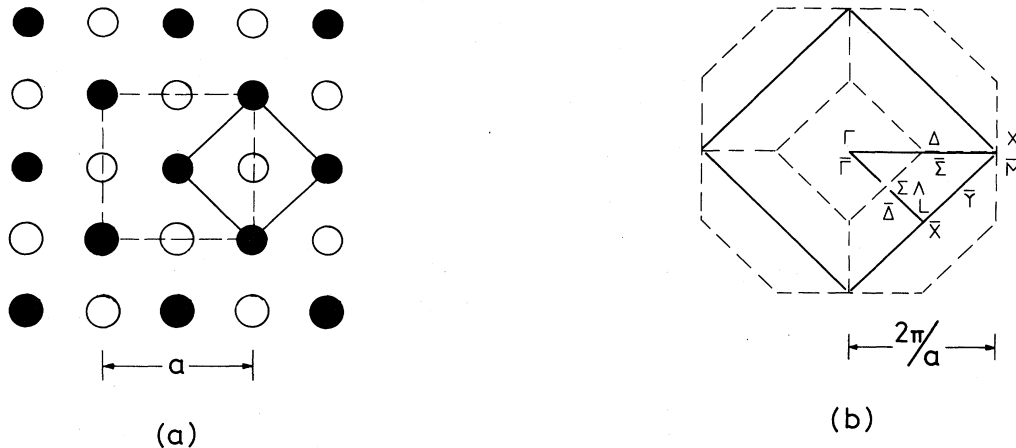


FIG. 4. (a) Top view of the (001) surface of fcc Ni. Solid circles represent atoms in the surface (S) layer and open circles in the subsurface ($S-1$) layer. The broken lines indicate the conventional cubic bulk unit cell and the lattice constant a is taken to be 6.6488 a.u. The solid lines show the surface unit cell. (b) Sketch of the projection of the three-dimensional Brillouin zone with the corresponding high-symmetry points and lines onto the two-dimensional Brillouin zone (solid lines) with the symmetry labels given for its irreducible part. The value of $2\pi/a$ is 1.79 \AA^{-1} .

compared with the conventional cubic bulk unit cell. Labels for wave functions such as d_{xy} , as used below, refer to the coordinate system of the conventional cubic bulk unit cell. As stated in our previous work,² the overall shape and the occurrence of surface states and surface res-

onances is very similar for the bands of the majority and the minority spin system (compare Figs. 5 and 7 and Figs. 6 and 8). Hence surface states and surface resonances are discussed for both spin systems simultaneously. In the band structures shown in Figs. 5–8, states whose wave

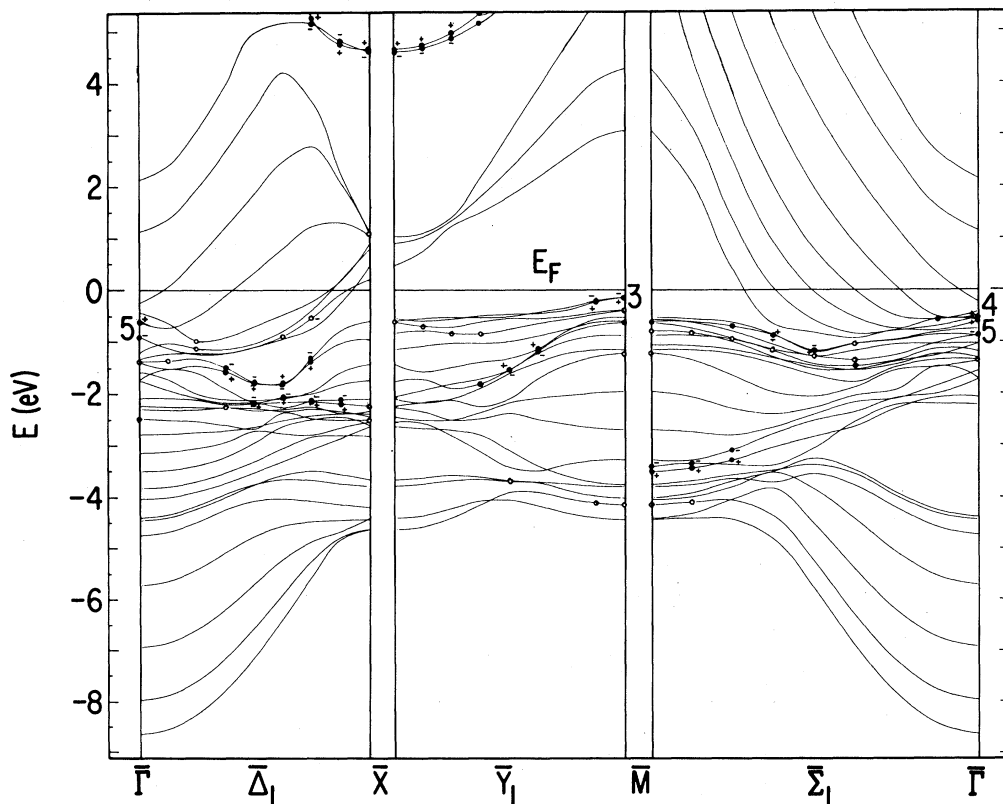


FIG. 5. Majority-spin energy bands for a seven-layer Ni(001) film for states with even symmetry with respect to symmetry planes perpendicular to the surface. Open circles indicate states whose wave functions have more than 80% weight within the surface and subsurface layers and solid circles denote states with more than 50% weight within the surface layer alone. (+) and (-) gives the parity with respect to a mirror reflection on a plane in the center of the film.

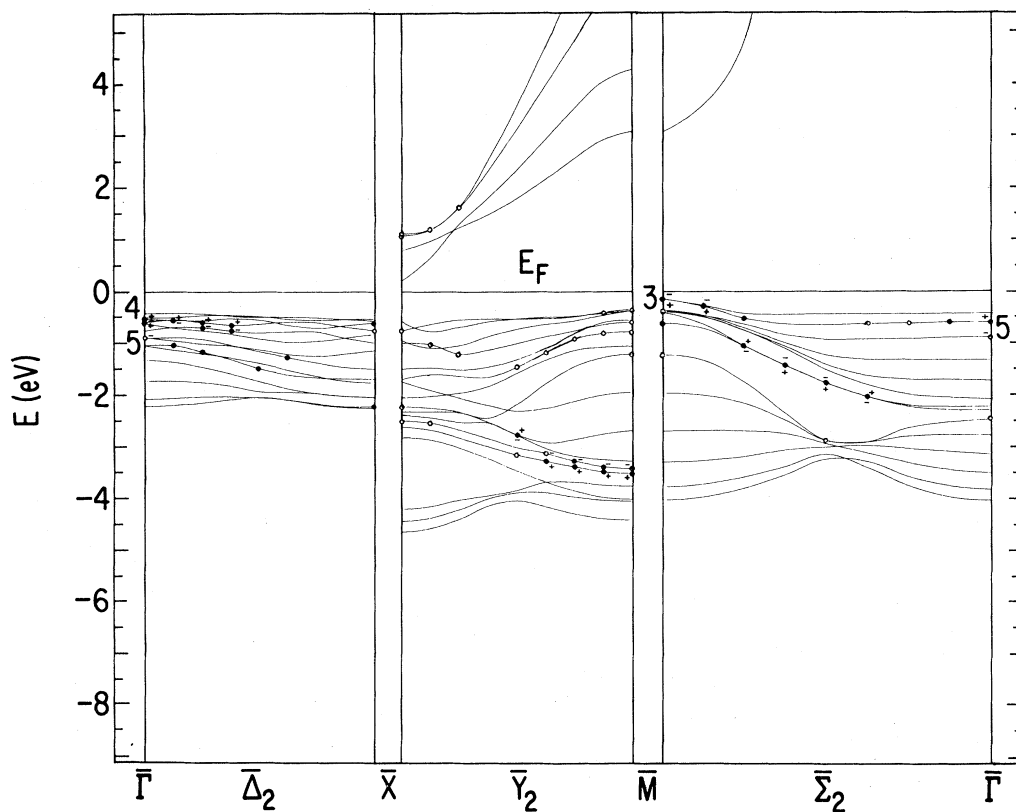


FIG. 6. Majority-spin energy bands for a seven-layer Ni(001) film for states which are odd with respect to symmetry planes perpendicular to the surface. Otherwise the same conventions are used as in Fig. 5.

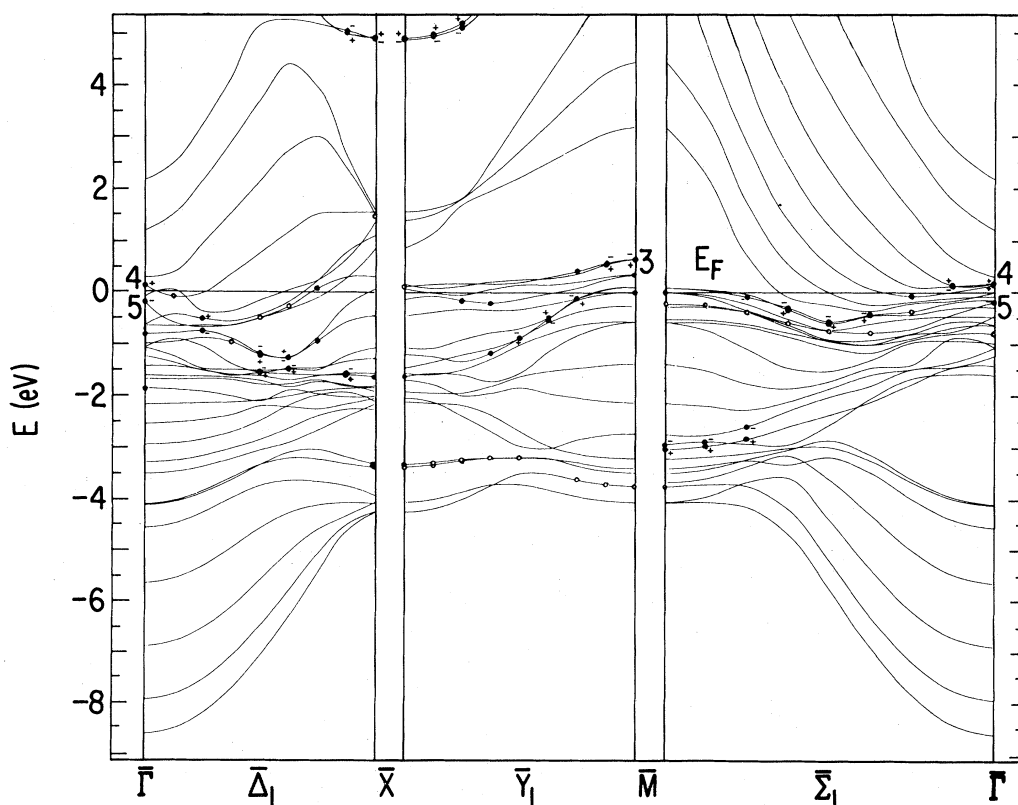


FIG. 7. Minority-spin energy bands for a seven-layer Ni(001) film for states which are even with respect to symmetry planes perpendicular to the surface. Otherwise the same conventions are used as in Fig. 5.

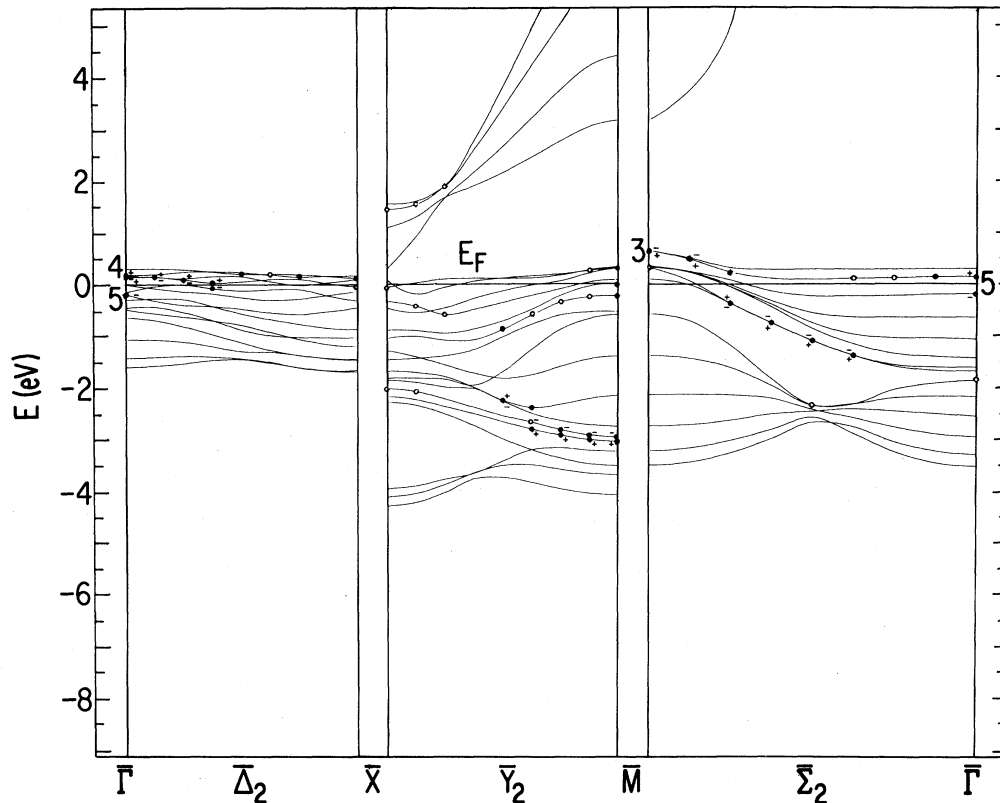


FIG. 8. Minority-spin energy bands for a seven-layer Ni(001) film for states which are odd with respect to symmetry planes perpendicular to the surface. Otherwise the same conventions are used as in Fig. 5.

function have a relative weight of more than 80% in the surface (S) and the subsurface ($S-1$) layer are indicated by circles. If this weight exceeds 50% for the surface layer alone, the circles are full. States which are extremely localized in the surface layer occur in nearly degenerate pairs of even and odd parity with respect to a mirror reflection in the center of the seven-layer slab. Such pairs are indicated in Figs. 5–8 by (+) and (–).

In Fig. 5 we show the energy-band structure for states of the majority-spin system which are even with respect to mirror planes, perpendicular to the (001) surface, containing the high-symmetry lines $\bar{\Delta}$, \bar{Y} , and $\bar{\Sigma}$. Similar to our previous calculations of five-layer slabs,² we find a free-electron-like surface state around \bar{X} , about 5 eV above the Fermi energy and just below the vacuum level. The exchange splitting of this state is about 0.25 eV.

One of the most striking surface states of the Ni(001) surface is an extremely localized state of \bar{M}_3 symmetry. Contrary to the results of earlier calculations^{1,6} we find the \bar{M}_3 majority surface state being occupied and 0.14 eV below the Fermi energy. In our previous five-layer calculations² this state was found to lie within 1 mRy of the Fermi level and the corresponding minority state 0.75 eV above E_F . In the present work we find this minority \bar{M}_3 surface state 0.64 eV above the Fermi level resulting in an exchange splitting of 0.78 eV in excellent agreement with the value of 0.75 eV found for the five-layer slab.² The origin of this \bar{M}_3 surface state is readily explained.^{22,23} This state is derived from bulk states of d_{xy} character

forming the top of the d band. Because of their d_{xy} character these states are highly localized within layers parallel to the surface. In bulk Ni these states are found²¹ to lie 0.33 eV below the Fermi energy for the majority-spin system and 0.37 eV above E_F for the minority-spin system. Our seven-layer slab calculation yields the corresponding bulklike states for the layers $S-1$, $S-2$, and the central layer 0.38 eV below and 0.34 eV above E_F , respectively. Owing to an electrostatic shift of the potential in the surface layer, this d_{xy} state splits off from the top of the d band and is shifted closer to the Fermi energy by 0.24 eV thus forming the highly localized surface state at \bar{M}_3 . As will be discussed below, this electrostatic shift also affects the core levels which have for the surface atoms a binding energy 0.3 to 0.5 eV less than for the corresponding bulk atoms. Away from the symmetry point \bar{M} the \bar{M}_3 surface state has a downward dispersion and joins into surface resonance states of \bar{Y}_1 and $\bar{\Sigma}_2$ symmetry fading out about $\frac{2}{3}$ of the way towards \bar{X} and $\bar{\Gamma}$, respectively (cf. Figs. 5–8). Very similar to the situation reported for the five-layer slab,² we find at $\bar{\Gamma}$ a surface state of $\bar{\Gamma}_4$ symmetry with the majority state 0.52 eV below and the minority state 0.18 eV above the Fermi level. This state disperses downwards away from $\bar{\Gamma}$ and joins into a $\bar{\Delta}_2$ and weak $\bar{\Sigma}_1$ surface resonance. Below the $\bar{\Gamma}_4$ surface state there exists a surface state of $\bar{\Gamma}_5$ symmetry (d_{xz}, d_{yz} character). The rather large splitting between the even (+) and odd (–) states of 0.29 eV even for the seven-layer film is an indication of the diffuse character of this

state. Between -1 and -2 eV we observe rather pronounced surface resonances of $\bar{\Delta}_1$ symmetry, mainly at k values between $\frac{1}{2}(\bar{\Gamma}\bar{X})$ and \bar{X} . Finally there exists a low-lying surface state of \bar{M}_4 symmetry, the majority and the minority states at 3.47 and 2.99 eV below the Fermi energy. The exchange splitting of 0.48 eV of this state at the bottom of the d band is thus seen to be markedly smaller than that of the d_{xy} states at the top of the d band. Away from \bar{M} this \bar{M}_4 surface state finds its continuation as surface resonances of $\bar{\Sigma}_1$ and \bar{Y}_2 symmetry with an upward dispersion. These resonances are pronounced about half the way from \bar{M} to \bar{X} and about a third the way along the $\bar{\Sigma}$. Owing to the increased film thickness used in the present calculations, the splitting of the (+) and (-) states for these surface resonances is clearly reduced compared with the results obtained for the five-layer film (compare Figs. 5–8 of the present work with Figs. 16–19

of Ref. 2).

The overall agreement of the surface band structure obtained with the FLAPW method for a seven-layer film is in remarkable agreement with our previous results for five-layer Ni(001) slabs where an earlier version of our LAPW method has been employed. In this earlier version, the nonspherical components of the potential inside the atomic spheres have been neglected. Such good overall agreement had been expected for the surface of a close-packed metal such as Ni. Nevertheless, sensitive details such as the question whether the majority \bar{M}_3 surface state is occupied or not can only be assessed by means of rigorous, highly accurate methods. As it turns out, both the early calculation of Wang and Freeman⁶ and the recent calculation by Jepsen *et al.*¹ find this state unoccupied.

Except for the location of the majority \bar{M}_3 surface state

TABLE V. Energies (in eV) of the core states in seven-layer Ni(001) film and surface-induced core-level shifts.

		Majority	Minority	Difference
S	1s	-8189.65	-8189.65	0.00
	2s	-976.59	-976.15	0.44
	2p _{1/2}	-852.59	-852.26	0.33
	2p _{3/2}	-835.16	-834.81	0.35
	3s	-107.82	-107.00	0.82
	3p _{1/2}	-70.13	-69.33	0.80
	3p _{3/2}	-67.92	-67.12	0.80
S-1	1s	-8190.03	-8190.03	0.00
	2s	-977.09	-976.68	0.41
	2p _{1/2}	-853.08	-852.77	0.31
	2p _{3/2}	-835.65	-835.33	0.32
	3s	-108.19	-107.44	0.75
	3p _{1/2}	-70.49	-69.76	0.73
	3p _{3/2}	-68.27	-67.55	0.72
S-2	1s	-8190.03	-8190.03	0.00
	2s	-977.09	-976.68	0.41
	2p _{1/2}	-853.08	-852.78	0.30
	2p _{3/2}	-835.60	-835.33	0.31
	3s	-108.18	-107.44	0.74
	3p _{1/2}	-70.48	-69.75	0.73
	3p _{3/2}	-68.26	-67.55	0.71
C	1s	-8190.01	-8190.01	0.00
	2s	-977.04	-976.66	0.38
	2p _{1/2}	-853.04	-852.75	0.29
	2p _{3/2}	-835.60	-835.30	0.30
	3s	-108.12	-107.42	0.70
	3p _{1/2}	-70.42	-69.74	0.68
	3p _{3/2}	-68.21	-67.53	0.68
	Difference (S)-(C)	Majority	Minority	
	1s	0.36	0.36	
	2s	0.45	0.51	
	2p _{1/2}	0.45	0.49	
	2p _{3/2}	0.44	0.49	
	3s	0.30	0.42	
	3p _{1/2}	0.29	0.41	
	3p _{3/2}	0.29	0.41	

with respect to the Fermi energy, the present highly precise LSDF band structures confirm the previous theoretical results^{1,2} and their relation to the experimental data obtained from angle-resolved photoemission experiments. In particular, the $\bar{\Delta}_1$ minority surface state reported by Plummer and Eberhardt²⁴ obviously cannot be related to any corresponding feature in the theoretical surface band structure (see Fig. 7) as was the case with previous *ab initio* local-spin-density-functional studies of the Ni(001) surface.^{1,2,6} Similarly, the surface state at $\bar{\Gamma}$ deduced from angle-resolved photoemission experiments by Erskine²⁵ has no evident theoretical counterpart in the ground-state energy-band structures.

F. Core-level shifts

In Table V we present the local-spin-density-functional one-particle energies for the core levels in a seven-layer Ni(001) film. As expected, the energy splitting between majority and minority states depends on the orbital character and ranges between 0 and 0.8 eV. The biggest splitting is found for the $3s$ and $3p$ states, obviously because of the large overlap with the valence $3d$ functions. It is interesting to note that for the $1s$ states no split is found.

In the bottom part of Table V the surface-induced core-level shifts are given in the form of differences between the energies of corresponding states in the surface (S) and the central (C) layers. In the surface layer we find a pronounced shift between 0.29 and 0.51 eV towards smaller binding energies. This shift, already mentioned in the discussion of the \bar{M}_3 surface state in the preceding section, can be understood² in terms of the following simple picture: As discussed in Sec. III D, the d band is narrower for the surface atoms than for bulklike atoms. Since for Ni the d band is more than half-filled, such a narrowing would cause a larger fraction of the d band to be occupied thus increasing the electronic charge for the surface atoms. This, however, appears to be energetically unfavorable and the filling of the d bands is counteracted by an electrostatic shift to smaller binding energies thus retaining the same amount of d -like charge also for the surface atoms (cf. Table I) and conserving layer-by-layer charge neutrality.

IV. SUMMARY AND CONCLUSIONS

We have presented the results of high-precision, self-consistent, all-electron local-spin-density-functional calculations using the full-potential linearized-augmented-plane-wave (FLAPW) method for a seven-layer Ni(001) film. It has been found that the magnetic moment for the

atoms in the surface layer is enhanced by almost 20% compared with the bulklike interior of the film. There is no indication of a Friedel-type oscillation in the magnetic moment on going from the surface into the interior of the metal. The subsurface atoms already have a moment close to the bulk value, so only one layer of surface atoms is found to be magnetically different from bulk Ni. This fact implies that a film of seven layers is sufficiently thick to assess questions of surface magnetism. For the contact spin densities at the nuclei we have obtained a negative polarization for all atoms where the magnitude is reduced for the surface atoms by about 20%. Furthermore it has been established that the contribution originating from the valence ($4s$ -derived) states changes sign for the surface atoms and becomes positive.

In agreement with angle-resolved photoemission spectra we find an occupied surface state of \bar{M}_3 symmetry of d_{xy} character which is split off from the top of the bulk d band due to an electrostatic shift of the potential for the surface atoms towards reduced binding energies. This state is continued by surface states and surface resonance states of $\bar{\Sigma}_2$ symmetry belonging to the majority-spin system. A pronounced downward dispersion away from \bar{M} has been obtained which does not agree with the photoemission results where no dispersion has been observed. The experimentally determined surface states of (minority) $\bar{\Delta}_1$ symmetry near the zone edge cannot be identified in the ground-state surface-band structure.

We have found a core-level shift between 0.3 and 0.5 eV towards reduced binding energies for the surface atoms. This effect is localized to the surface atoms and the subsurface atoms behave in a bulklike manner. This surface-induced shift has been shown to be related to the d -band narrowing for the surface atoms combined with layer-by-layer charge neutrality.

It is important to conclude that the present calculations on seven-layer Ni(001) slab confirm to a large extent the results of earlier calculations made for films with only five layers and involving approximations in dealing with the full potential thus providing, *a posteriori*, a justification and an assessment of the approximations made in these earlier studies.

ACKNOWLEDGMENTS

Research at Northwestern University was supported by the National Science Foundation (Grant No. DMR-82-16543). Research at the College of William and Mary was supported by the National Science Foundation (Grant No. DMR-81-20550).

*Permanent address: Institut für Physikalische Chemie, Universität Wien, Währingerstrasse 42, A-1090 Vienna, Austria.

¹O. Jepsen, M. Madsen, and O. K. Andersen, *J. Magn. Magn. Mater.* **15-18**, 867 (1980); *Phys. Rev. B* **26**, 2790 (1982).

²H. Krakauer, A. J. Freeman, and E. Wimmer, *Phys. Rev. B* **28**, 610 (1983).

³R. Feder, S. F. Alvarado, E. Tamura, and E. Kisker, *Surf. Sci.* **127**, 83 (1983).

⁴For detailed references the reader is referred to those given in Refs. 1 and 2.

⁵R. Clauberger, H. Hopster, and R. Raue, *Phys. Rev. B* **29**, 4395 (1984).

⁶C. S. Wang and A. J. Freeman, *Phys. Rev. B* **21**, 4585 (1980).

⁷P. Hohenberg and W. Kohn, *Phys. Rev.* **136**, B864 (1964).

⁸W. Kohn and L. J. Sham, *Phys. Rev.* **140**, A1133 (1965).

⁹U. von Barth and L. Hedin, *J. Phys. C* **5**, 1629 (1972).

- ¹⁰O. Gunnarsson, B. I. Lundqvist, and S. Lundqvist, *Solid State Commun.* **11**, 149 (1972).
- ¹¹E. Wimmer, H. Krakauer, M. Weinert, and A. J. Freeman, *Phys. Rev. B* **24**, 864 (1981), and references therein.
- ¹²M. Weinert, W. Wimmer, A. J. Freeman, and H. Krakauer, *Phys. Rev. Lett* **47**, 705 (1981).
- ¹³D. G. Anderson, *J. Assoc. Comp. Mach.* **12**, 547 (1964).
- ¹⁴D. R. Hamann (private communication).
- ¹⁵E. Wimmer, A. J. Freeman, M. Weinert, H. Krakauer, J. R. Hiskes, and A. M. Karo, *Phys. Rev. Lett* **48**, 1128 (1982).
- ¹⁶B. G. Baker, B. B. Johnson, and G. L. C. Maire, *Surf. Sci.* **24**, 572 (1971).
- ¹⁷W. Eib and S. F. Alvarado, *Phys. Rev. Lett.* **37**, 444 (1976).
- ¹⁸C. Rau, *J. Magn. Magn. Mater.* **30**, 141 (1982).
- ¹⁹H. Dannan, R. Herr, and A. J. P. Meyer, *J. Appl. Phys.* **39**, 669 (1968). In the value of 0.56 the orbital contributions has already been subtracted. Tacitly it is assumed that this orbital contribution to the total magnetic moment remains unaltered at the surface.
- ²⁰A. J. Freeman and R. E. Watson, in *Magnetism*, edited by G. T. Rado and H. Suhl (Academic, New York, 1964), p. 167.
- ²¹V. L. Moruzzi, J. F. Janak, and A. R. Williams, *Calculated Electronic Properties of Metals* (Pergamon, New York, 1978).
- ²²F. J. Arlinghaus, J. G. Gay, and J. R. Smith, *Phys. Rev. B* **21**, 2055 (1980).
- ²³J. E. Inglesfield, *Rep. Prog. Phys.* **45**, 223 (1982).
- ²⁴E. W. Plummer and W. Eberhardt, *Phys. Rev. B* **20**, 1444 (1979).
- ²⁵J. L. Erskine, *Phys. Rev. Lett.* **45**, 1446 (1980).